Radiative muon capture in medium heavy nuclei in a relativistic mean field theory model

Harold W. Fearing
TRIUMF, 4004 Wesbrook Mall, Vancouver, British Columbia, Canada V6T 2A3

Mark S. Welsh
Department of Physics and Astronomy, University of Victoria, Victoria, British Columbia, Canada V8W 3P6
(Received 17 December 1991)

Radiative and ordinary muon capture are studied in medium heavy nuclei using a relativistic mean field theory approach. A relativistic Fermi gas model is used to describe the nucleus and the local density approximation, together with realistic density distributions, are used to relate the process in infinite nuclear matter to finite nuclei. A number of density dependent effects not considered in previous nonrelativistic calculations are considered, as, for example, the variation of the effective nucleon mass and of the Fermi momentum with the nuclear density. The photon spectrum and the total experimentally accessible radiative rate (i.e., the part of the spectrum with photon momentum $k \geq 57$ MeV) are calculated for a variety of nuclei, along with the ordinary muon capture rate. The aim is to understand the sensitivities to the various components and to assess the reliability of such models for extracting the induced pseudoscalar coupling constant g_P from the experimental data. We find that the rates are quite dependent on the various inputs, which suggests that it will be difficult to extract g_P and casts some doubt on the validity of previous similar calculations. Some interesting qualitative features emerge from a comparison with recent data, however. The absolute rates are too high, which is consistent with other calculations. However, the model does reproduce rather well the Z dependence of both relative and absolute radiative rates without requiring any quenching of g_p in heavy nuclei. Furthermore the model gives an enhancement in the spectrum near the end point as compared to the uniform density model. Such an enhancement seems to be suggested by the data.

PACS number(s): 23.40.Bw, 13.10.+q, 13.40.Ks

I. INTRODUCTION

The radiative muon capture (RMC) process, $\mu p \rightarrow n\nu_\mu\gamma$, is a useful laboratory for the determination of the induced pseudoscalar coupling constant of the weak interaction, g_P. Due to the very low rate for this process as compared to ordinary, nonradiative, muon capture (OMC) most recent experimental data available [1–7] come from medium heavy nuclei, although the first experiment measuring radiative muon capture on a free proton is in progress at present [8]. Therefore calculations must be extended to finite nuclei, with the additional theoretical complexity which this entails. Potentially there may also be some new physical effects such as renormalization of the coupling constants in nuclear matter. Recent calculations include those of Refs. [9–11] and a review of theoretical and experimental work can be found in Ref. [12].

From another point of view radiative muon capture was used by Fearing and Walker [9] as a testing ground for the relativistic mean field theories [13] which have generated so much interest in areas such as proton nucleus scattering. There the RMC rate was calculated completely relativistically using the mean field theory and a Fermi gas model for infinite nuclear matter and the results suggested the possibility of some interesting effects appearing in finite nuclei.

Thus the aim of the present calculation is twofold. We wish to extend to finite nuclei this relativistic mean field theory approach to radiative muon capture. We also want to see if such a model can adequately describe some of the general trends of the experimental data.

Our general technique depends on the local density approximation. We interpret the result of Ref. [9] in nuclear matter as giving the capture rate as a function of the density. This rate is then folded over a realistic nuclear density. Such an approach bypasses some of the complications of a rigorous relativistic calculation. The mean fields are still constants so that the states are still plane waves and thus there will be no nuclear structure effects arising from the wave functions. Also, the problems with gauge invariance generated by spatially varying fields are avoided. Thus the nuclear model is somewhat simplistic, but may be expected to provide at least qualitative information about the variation of the radiative rate with atomic number Z, and with different values of the coupling constant g_P.

Section II gives a brief review of the methods used to calculate ordinary and radiative capture rates on a free proton and Sec. III reviews the application of the Fermi gas model to infinite nuclear matter. The implications of the local density approximation and details of the nuclear model for finite nuclei are introduced in Sec. IV. Section V gives results for the RMC rate and photon spectrum

and for the OMC rate, using a variety of assumptions about the various ingredients. A comparison with other, mainly nonrelativistic, approaches to this problem is also made.

In the final section, Sec. VI, some conclusions are drawn about the quantitative accuracy of this and other similar models, and about the implications for the extraction of the induced pseudoscalar coupling constant from radiative muon capture data.

II. RMC ON A PROTON

In this section and the next we review the ingredients of the basic RMC process and of the relativistic mean field theory—Fermi gas model used in Ref. [9] to get the capture rates in infinite nuclear matter. Further details and notation can be found in that reference.

As is usual in the theory of radiative muon capture, we begin with a set of Feynman diagrams (shown in Fig. 1). These are the standard diagrams for this process as used in Ref. [14] and in most subsequent calculations, e.g., Refs. [9, 15, 16]. Additional diagrams resulting from the $\Delta(1232)$ resonance are not included, due to their small contribution to the statistical rate [17, 18]. The included diagrams give rise to an amplitude which is squared and converted to a rate in the standard fashion. The amplitude we use is given explicitly in Ref. [15].

The weak vertex factor of the nucleon is initially taken to be of the general form

$$\Gamma^\alpha(q) = g_V\gamma^\alpha + \frac{ig_M}{2m_p}\sigma^{\alpha\beta}q_\beta + \frac{g_S}{m_\mu}q^\alpha + g_A\gamma^\alpha\gamma_5 + \frac{g_P(q^2)}{m_\mu}q^\alpha\gamma_5 + \frac{ig_T}{2m_p}\sigma^{\alpha\beta}q_\beta\gamma_5. \quad (1)$$

We assume that the second class induced scalar and tensor couplings g_S and g_T are zero, and take the vector, axial vector, and weak magnetism couplings to be independent of the four-momentum transfer squared q^2 with values $g_V = 1$, $g_A = -1.25$, and $g_M = 3.71$.

Only the induced pseudoscalar coupling constant, whose value we wish to determine, is thought to vary greatly within the range of q^2 available. Its dependence upon q^2 is taken to be

$$g_P(q^2) = g_P(-m_\mu^2)\frac{m_\pi^2 + m_\mu^2}{m_\pi^2 - q^2}, \quad (2)$$

where

$$g_P(-m_\mu^2) = \frac{m_\mu(m_p + m_n)}{m_\pi^2 + m_\mu^2}g_A \quad (3)$$

is the Goldberger-Treiman value [19].

Two momentum transfers enter the expression for the amplitude of radiative muon capture. The first, $q_L \equiv n - p$ (where n, p, μ, ν, and k represent the four-vectors associated with the neutron, proton, muon, neutrino, and photon), enters in Figs. 1(a), 1(d), and 1(e). It takes on a value $q_L^2 \approx -m_\mu^2$ in the region where the photon momentum is large. This is the region of experimental interest since the photon spectrum can only be measured experimentally for k greater than about 55–60 MeV. So we see that $g_P(q_L^2)$ remains near the Goldberger-Treiman value. However, the other momentum transfer $q_N \equiv n - p + k$ [appearing in Figs. 1(b), 1(c), and 1(d)] can take on a value $q_N^2 \approx +m_\mu^2$ for large k. This produces an enhancement in $g_P(q_N^2)$, greatly increasing the contribution of the induced pseudoscalar coupling constant to the radiative rate in the region of interest.

Due to the complexity of the problem, the squaring of the matrix element and the summing over spins, which are necessary to obtain the rates, are carried out entirely numerically. More details of this procedure are given in Ref. [15].

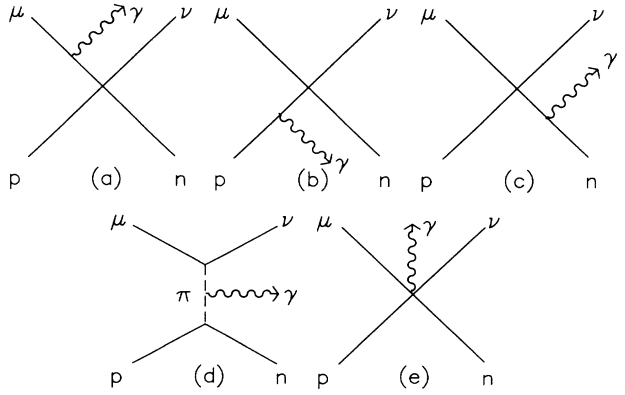

FIG. 1. Feynman diagrams contributing to radiative muon capture on a proton.

III. RELATIVISTIC MEAN FIELD THEORY: FERMI GAS MODEL

In the relativistic mean field theory approach [13] it is supposed that a renormalization of the nucleon masses occurs in the nuclear medium. In this model the effects of the nuclear medium are described by large scalar and vector mean fields. For infinite nuclear matter these fields are constants. The presence of such constant fields in the Dirac equation for a nucleon has an effect equivalent to using the free Dirac equation with a renormalized nucleon mass $m^* = m - G_S\phi_0$ where, ϕ_0 is the mean scalar field and G_S is a coupling. The effects of the mean vector field appear only as a phase factor in the wave function in this simple model. A typical value for the potential due to the scalar field is $G_S\phi_0 = 400$ MeV [13] leading to a value for the effective nucleon mass of $m^* = 0.57m$.

Thus for infinite nuclear matter the states are just the free Dirac plane waves with $m \to m^*$, and with an additional time dependent phase factor depending on the vector potential which, however, cancels in all matrix elements. Thus one can calculate the matrix elements by simply replacing m with m^* everywhere in the free proton expressions. This change from the free nucleon mass to the renormalized mass m^* was performed consistently throughout this calculation, including the Goldberger-Treiman relation for g_P, Eq. (3), and the kinematics

defining the allowed phase space for the ordinary and radiative capture rates. The free proton mass m_p was retained in the weak magnetism term $g_M/2m_p$ of Eq. (1), however, as there it simply defines the units.

Within the context of the simple model we use here the replacement $m \to m^*$ in Eq. (3) for g_P follows directly and rigorously from the assumption of partially conserved axial-vector current and the usual steps for deriving the Goldberger-Treiman relation for the free case. In the derivation the only difference from the free case is that now the nucleon states satisfy the Dirac equation with $m \to m^*$ and an extra term involving the mean vector field (Eq. (1) of Ref. [9]) rather than the free Dirac equation. The vector terms cancel when this equation is used to replace the derivatives by masses and one is left with the same expression as the free case, except with $m \to m^*$. This does not of course exhaust the possible changes in g_P induced by the nuclear medium. For example, nothing is included to account for the pion propagating in the medium. Such effects could change the effective value of g_P and certainly should be considered in the next stage of calculations.

To apply this to infinite nuclear matter, and ultimately finite nuclei, we assume a Fermi gas model. This model supposes that in the initial state all of the nucleon momentum states up to a certain value (the Fermi momentum, k_F) are filled, and that no higher states are excited. Hence in muon capture the initial proton state must have a momentum less than the proton Fermi momentum, and, due to the Pauli exclusion principle, the final state neutron must have a momentum greater than the neutron Fermi momentum. The Fermi momenta depend on the proton and neutron densities ρ_p and ρ_n via

$$k_{F_{p,n}} = (3\pi^2 \rho_{p,n})^{\frac{1}{3}}. \tag{4}$$

The capture rate on a single proton of momentum p is then integrated over all $p \leq k_{F_p}$, with the constraint $n \geq k_{F_n}$. The resulting expressions for the ordinary (nonradiative) and radiative muon capture rates in infinite nuclear matter with density determined by $k_{F_{p,n}}$ as taken directly from Ref. [9] are

$$\Gamma_{\rm ord} = G_F^2 \frac{3m_p m_n}{4\pi k_{F_p}^3} |\phi_\mu(0)|^2 \int_{p_{\rm min}}^{k_{F_p}} dp \int_{k_{F_n}}^{n_{\rm max}} dn \frac{E_\nu n p^2}{E_p E_n \mid \mathbf{n} + \boldsymbol{\nu} \mid} \frac{1}{4} \sum_{\rm spins} |M_{\rm fi}^{\rm ord}|^2, \tag{5}$$

$$\Gamma_{\rm rad} = \frac{G_F^2 \alpha}{4\pi^2} \frac{3m_p m_n}{4\pi k_{F_p}^3} |\phi_\mu(0)|^2 \int_{k_{\rm min}}^{k_{\rm max}} dk \int_{(\cos\theta_k)_{\rm min}}^{(\cos\theta_k)_{\rm max}} d\cos\theta_k \int_{p_{\rm min}}^{k_{F_p}} dp \int_{k_{F_n}}^{n_{\rm max}} dn \int_0^{2\pi} d\phi_n \frac{E_\nu n p^2 k}{E_p E_n \mid \mathbf{n} + \boldsymbol{\nu} \mid} \frac{1}{4} \sum_{\rm spins} |M_{\rm fi}^{\rm rad}|^2. \tag{6}$$

Here, $G_F = 1.137 \times 10^{-11}$ MeV^{-2} is the Fermi constant, and α is the fine-structure constant. At this point, we have introduced the muon density using the usual approximation for finite nuclei, that is, by extracting the muon wave function from the matrix element and evaluating it at the origin.

Note that these give the rate *per proton* so a sum over initial proton states will introduce a factor Z into both the ordinary and radiative capture rates.

IV. APPLICATION TO FINITE NUCLEI

To apply the above formalism to finite nuclei we use the local density approximation. In this approach the rates given above are considered to be functions of the density, $\Gamma(\rho_p, \rho_n)$, via their dependence on $k_{F_{p,n}}$ which are related to the densities by Eq. (4). We thus multiply the rate per proton by the nuclear proton density, i.e., the number of protons per unit volume, $\rho_p(r)$, and integrate over the volume. Schematically

$$\Gamma = \int d^3r \, \Gamma(\rho_p, \rho_n) \rho_p(r). \tag{7}$$

This local density approximation is often used in a variety of circumstances. A discussion of its validity for muon capture is given in Ref. [20].

For the nuclear density we used a two-parameter Fermi-Dirac density distribution,

$$\rho(r) = \frac{\rho_0}{1 + \exp(\frac{r - R_0}{A_0})} \tag{8}$$

with the half-density radius R_0 and the skin thickness A_0 taken from electron scattering data [21] where available, with the rest being computed using the fits to such data given in Ref. [22]. The density function $\rho(r)$ is normalized to one so that $\rho_p = Z\rho(r)$ and $\rho_n = (A - Z)\rho(r)$. We also investigated the uniform nuclear charge distribution which has often been used. It can be obtained as a special case of Eq. (8) by letting $A_0 \approx 0$. One must also replace R_0 by $R_{\rm eq}$, which is the equivalent radius for a spherical, uniform density nucleus. The parameters used are given in Table I.

The nuclear charge distribution was assumed to apply, when suitably normalized, to both protons and neutrons, thus allowing a calculation of k_{F_p} and k_{F_n}.

Some important caveats to this approach as applied to finite nuclei should be mentioned. First the mean field theory for infinite nuclear matter assumes an equal number of protons and neutrons. It is necessary to assume here, as has been done in other applications of this approach, that no major change occurs in applying this to finite nuclei with $N \neq Z$. Also the model does not include effects of pion propagation. Such effects could affect g_P

TABLE I. Data used in the computation of ordinary and radiative capture rates. The radius $R_{\rm eq}$ is the equivalent radius of a spherical, uniform density nucleus. The muon binding energy $E_{\mu B}$, $R_{\rm eq}$, and $Z_{\rm eff}$ are taken from Refs. [23,24]. A_0 and R_0 come from Ref. [21] and the Coulomb energy E_C comes from Eq. (11). ΔM is the energy difference between the ground states of the initial and final nuclei. $E_{\mu B}$, E_C, and ΔM are in MeV while $R_{\rm eq}$, R_0, and A_0 are in fm.

	$E_{\mu B}$	E_C	$R_{\rm eq}$	$Z_{\rm eff}$	A	R_0	A_0	ΔM
$_{6}$C	0.10011	2.45	3.87	5.72	12	2.35	0.52	13.88
$_{8}$O	0.17779	3.23	4.01	7.49	16	2.61	0.51	10.93
$_{13}$Al	0.4629	4.83	4.47	11.48	27	2.95	0.54	3.12
$_{14}$Si	0.5345	5.16	4.52	12.22	28	3.06	0.55	5.15
$_{20}$Ca	1.0533	6.69	5.03	16.15	40	3.51	0.56	1.82
$_{26}$Fe	1.7158	8.47	5.20	19.59	56	3.97	0.59	4.21
$_{28}$Ni	1.9645	9.15	5.19	20.66	58	4.11	0.56	0.89
$_{42}$Mo	3.963	12.61	5.68	26.37	96	4.92	0.55	3.70
$_{50}$Sn	5.233	14.19	6.02	28.64	120	5.32	0.58	5.81
$_{64}$Gd	7.505	16.48	6.65	31.34	158	5.89	0.55	3.99
$_{74}$W	9.160	18.13	7.00	32.76	184	6.51	0.54	3.38
$_{82}$Pb	10.657	19.96	7.05	34.18	208	6.62	0.55	5.51
$_{83}$Bi	10.715	19.67	7.24	34.00	209	6.75	0.47	1.15
$_{92}$U	12.250	21.06	7.50	34.94	238	6.81	0.61	4.12

and contribute to various exchange corrections. Finally, it is becoming clear that higher order corrections to this simple model are important. Despite these caveats, however, we expect the model to provide a simple approach, consistent with other applications, which will give at least qualitatively some of the general aspects of the process.

A number of other features become important when one goes from infinite to finite nuclei. We list these here with a description of our standard choice together with some of the other options which will be investigated numerically in the next section.

In first approximation the muon wave function evaluated at the origin may now be replaced by an average over the extent of the nucleus, as has been done in many previous calculations:

$$|\phi_\mu(0)|^2 \to \overline{|\phi_\mu(0)|}^2 = \frac{(m_\mu^r \alpha)^3}{\pi} \frac{Z_{\rm eff}^4}{Z}, \tag{9}$$

where m_μ^r is the muon reduced mass. The extra factor $(Z_{\rm eff}/Z)$ in this equation originates from the definition of $Z_{\rm eff}$, which includes the Z present in ρ_p. The values of the quantity $Z_{\rm eff}$ are taken from Ford and Wills [23], and reflect their calculation of the overlap of a very accurate muon wave function with the nuclear density. If the rate $\Gamma(\rho_p, \rho_n)$ in Eq. (7) depends on r only via the muon wave function, then the weighting of $|\phi_\mu(r)|^2$ is the same as that used for the calculation of $Z_{\rm eff}$, namely, $\rho_p(r)$, and we would expect this to be a good approximation. However if $\Gamma(\rho_p, \rho_n)$ depends on r via a dependence on k_F, for example, then the weighting is different and the approximation may not be so good.

Within our calculation, however, it is very easy to put the square of the muon wave function under the integral on r, i.e., to use $|\phi_\mu(r)|^2$ instead of $|\phi_\mu(0)|^2$ in Eqs. (5)–(7) and thus bypass some of the approximations involved in using $Z_{\rm eff}$. As a simple test case, this was done for ^{208}Pb using a Bohr wave function to calculate $Z_{\rm eff}$ and compared to the result when this same simple wave function is put under the integral. The two approaches differed substantially. It thus appears that putting a reasonably accurate muon wave function under the radial integration is a necessity, at least when a nonuniform nuclear distribution is used since in that case the approximation that the rate is nearly constant over the extent of the nucleus is not well justified. Consequently a set of nonrelativistic $1S$ wave functions for the potential corresponding to the Fermi charge distribution used for each nucleus was calculated numerically by solving the Schrödinger equation using a fourth order Runge-Kutta integrator method. These wave functions, placed inside the radial integration, were used in our final results.

Two other effects are quite important, those due to the muon binding energy $E_{\mu B}$ and to the proton Coulomb energy E_C. Since E_C is released when the proton changes into a neutron and $E_{\mu B}$ must be provided when the muon is captured, it is the difference $E_C - E_{\mu B}$ which is important. The results are sensitive to this quantity because it affects the maximum energy available for the photon or neutrino and both RMC and OMC are very sensitive to this maximum energy.

In the phase space, the introduction of these two energies just changes the energy conserving delta function to $\delta(m_\mu - E_{\mu B} + E_p + E_C - E_n - \nu - k)$, where E_p and E_n are the on-shell energies ($E^2 = p^2 + m^2$) of the proton and neutron. Thus, for the *phase space only*, one can simply replace $m_\mu \to m'_\mu = m_\mu - E_{\mu B} + E_C$.

However, this is not the correct replacement in the matrix element, for rather subtle reasons. Within the context of the relativistic mean field theory we can treat the Coulomb energy for both muon and proton as an additional field, which we take as constant, appearing in the Hamiltonian, in parallel with the treatment of the mean vector field. Then using arguments [9] exactly analogous to those showing that the vector field does not appear in the propagators, one shows that the Coulomb fields also do not appear in the propagators. Similarly $E_{\mu B}$ does not appear in the muon propagator. The other factor

which enters is $q \sim n-p$, which appears in the weak vertex function. In going from the coordinate space derivative represented by p to momentum space, one brings down a factor involving E_C. In the analogous case of the strong vector field a similar factor coming from n cancels that from p. Here, however, this second factor does not arise and the E_C survives. One can now use the conservation of four-momentum to eliminate it in favor of $E_{\mu B}$. The end result is that the matrix element is evaluated everywhere with physical masses and four-vector momenta satisfying the conservation equations, that E_C appears nowhere explicitly, and that $E_{\mu B}$ appears only in the momentum transfers $q_L \to m_\mu - E_{\mu B} - k - \nu$ and $q_N \to m_\mu - E_{\mu B} - \nu$.

In our calculations the $1S$ muon binding energy $E_{\mu B}$ was taken from the relativistic solutions of Ford and Wills [23]. Initially the proton Coulomb energy was taken as a constant derived by assuming that the nucleus was a sphere of radius $R_{\rm eq}$ with an initially uniform charge density, becoming a final state which is identical except for a missing spherical shell of charge representing the missing proton. The Coulomb energy obtained by averaging over all protons is then

$$E_C = \frac{3\alpha Z}{2R_{\rm eq}}\left(\frac{7}{5} - \frac{1}{Z^{5/3}}\sum_{N=1}^{Z} N^{\frac{2}{3}}\right). \tag{10}$$

This result is essentially identical to that obtained by taking the difference in total Coulomb energies of uniform spheres of charge Z and $Z-1$, i.e.,

$$E_C = \frac{3\alpha}{5R_{\rm eq}}(2Z-1). \tag{11}$$

Other choices, for example, taking the result from the semiempirical mass formula or requiring, as suggested in Ref. [25], that $m_\mu - E_{\mu B} + m_p - m_n + E_C \approx 113$ MeV, gave very similar results.

It would perhaps be more consistent with the local density approximation to use a Coulomb energy which changes with r across the nucleus, as, for example,

$$E_C \to E_C(r) = Z\alpha \int d^3r' \frac{\rho(r')}{|\,\mathbf{r}-\mathbf{r}'\,|}, \tag{12}$$

which can be calculated numerically for any assumed charge distribution $\rho(r)$. For the uniform distribution this gives the familiar form

$$E_C(r) = \frac{3Z\alpha}{2R_{\rm eq}^3}\left(R_{\rm eq}^2 - \frac{r^2}{3}\right). \tag{13}$$

However because of the considerations of the next paragraph, this would not change our results and so we used only the constant value of E_C given by Eq. (11).

For realistic finite nuclei the Coulomb energy is not the only energy which differs from initial to final state. There are other isospin dependent pieces, one being the so-called symmetry energy, which contribute to the difference between the mass of initial nucleus $M(Z)$ and that of the ground state of the final one $M(Z-1)$. It is important that this mass difference $\Delta M = M(Z-1) - M(Z)$ be correct as this affects the amount of energy available and the phase space. It is not clear how to include such energy consistently within the mean field theory so what we did was simply replace $E_C \to E_C - \Delta E$ in the energy conserving delta function which defines the phase space and kinematic quantities. The quantity ΔE was fixed by the requirement that the energy difference between the initial state and the lowest final state be ΔM which was taken from experimental information on nuclear masses and is given in Table I. Thus we require $\Delta M = \sqrt{k_{F_n}^2 + m_n^{*2}} - \sqrt{k_{F_p}^2 + m_p^{*2}} - E_C + \Delta E$ for all values of r. For most nuclei this is a relatively large effect and ΔE cancels a large portion of E_C. This procedure does ensure that the overall maximum photon energy is correct, which is very important given the sensitivity of the rates to this energy. It also amounts to ensuring that the Q value in our calculation is correct. Note that it is ΔM which fixes the energy available. Thus the specific details of the choice of E_C or of m^* do not matter for the phase space, as ΔE is always adjusted to give the correct final Q value, i.e., of ΔM.

Finally in principle m^* has a dependence on the Fermi momentum as calculated self-consistently in mean field theory [13, 26]. This is reflected in a dependence on nucleon number density within the nucleus and thus on the radius in the local density approximation.

Before looking at the results we summarize some of the checks we performed to verify the correctness of the numerical computations. As is usual checks were made on the stability of the integrals by varying the number of integration points. The kinematics were reworked in several ways, and the resulting four-vectors were always checked for four-momentum conservation. The amplitudes were routinely checked for gauge invariance, and this in fact proved a very useful tool in understanding how to put E_C and $E_{\mu B}$ into the matrix elements. For a uniform charge distribution with $E_C = E_{\mu B} = 0$ the results should reduce to those of Ref. [9], after proper account is taken of the differences in $Z_{\rm eff}$ and the rate is converted to rate per proton. This was found to be the case.

We also checked that in the limit $k_{F_{p,n}} \to 0$, $Z = A = 1$, and $E_{\mu B} = 0.00253$ MeV, the results reduced to those of Ref. [15] for muon capture on a free proton. As an additional check, an exact analytic expression for ordinary muon capture on a proton was computed (the invariant amplitude squared being found to be the same as that given by Ref. [20]) and this was compared with the numerical calculation. The results were the same to within $\sim 1.5\%$.

V. RESULTS

The OMC rate $\Gamma_{\rm OMC}$, the RMC photon spectrum $d\Gamma/dk$, the radiative rate $\Gamma(\geq 57)$, which is defined as the radiative spectrum integrated over photon energies greater than 57 MeV, and the relative rates $dR/dk = (d\Gamma/dk)/\Gamma_{\rm OMC}$ and $R(\geq 57) = \Gamma(\geq 57)/\Gamma_{\rm OMC}$, have all been calculated for a variety of medium heavy nuclei ranging from ^{40}Ca to ^{208}Pb. We first want to understand the sensitivity to the various ingredients and ways

TABLE II. Ordinary capture rates Γ_{OMC} in units of 10^6 s^{-1} for a variety of nuclei. The numbered columns correspond to the various options described in the text. Options 1–6 are independent of the form of the nuclear density, and 7–9 are given for the two-parameter Fermi-Dirac density distribution. For a uniform distribution options 7 and 8 are not relevant and 9 is the same as 6. Nuclei lighter than ^{40}Ca are included for reference only, as our model is not expected to be applicable for such nuclei.

	1	2	3	4	5	6	7	8	9
$_{6}$C	0.0490	0.0380	0.0751	0.0749	0.0805	0.0492	0.0550	0.0613	0.0602
$_{8}$O	0.145	0.113	0.204	0.203	0.223	0.147	0.167	0.184	0.179
$_{13}$Al	0.807	0.626	0.932	0.919	1.07	0.900	1.01	1.08	1.03
$_{14}$Si	1.04	0.804	1.32	1.30	1.51	1.13	1.29	1.40	1.33
$_{20}$Ca	3.17	2.46	3.97	3.85	4.69	3.72	4.08	4.39	4.09
$_{26}$Fe	6.89	5.34	6.05	5.73	7.54	5.83	7.21	7.71	6.97
$_{28}$Ni	8.52	6.61	8.31	7.83	10.4	8.29	10.1	10.8	9.79
$_{42}$Mo	22.7	17.6	13.0	11.3	17.8	13.8	18.4	19.4	16.7
$_{50}$Sn	31.6	24.5	13.7	11.1	19.6	14.5	20.7	21.9	18.1
$_{64}$Gd	45.3	35.1	17.4	12.5	25.5	19.3	26.0	27.1	21.7
$_{74}$W	54.1	42.0	20.0	13.1	29.6	21.6	30.4	32.2	25.8
$_{82}$Pb	64.1	49.7	18.6	10.8	28.8	18.8	28.3	29.7	22.7
$_{83}$Bi	62.8	48.7	20.9	12.4	31.5	24.4	32.3	33.6	27.0
$_{92}$U	70.0	54.3	19.2	9.85	29.6	19.8	29.5	30.9	22.3

of including certain effects and so have given the OMC rate and $\Gamma(\geq 57)$ for a number of different options. We have considered the uniform nuclear charge distribution and the radially varying Fermi-Dirac distribution form as different models, though many of the effects are in fact independent of the particular density chosen. Results for the ordinary, nonradiative, capture rate are given in Table II and those for the radiative rates in Tables III and IV.

We describe below the various options which we considered. Each option builds on the preceding ones, with only the changes noted. The intent is to start with the simplest case and build towards our final result, adding only one ingredient at a time, so as to understand the sensitivities of the result to the various ingredients and choices.

For options 1–6, $\Gamma(\rho_p, \rho_n)$ is independent of r so that the result is independent of the nuclear density distribution, as can be seen from Eq. (7). In option 9 an explicit r dependence is introduced in $\Gamma(\rho_p, \rho_n)$ via the r dependence of the muon wave function, so this option is relevant for both the uniform and radially varying densities. However for the uniform density, since there is no other r dependence, option 9 will be the same as option 6, by virtue of the definition of Z_{eff}. Options 7 and 8 generate an r dependence in $\Gamma(\rho_p, \rho_n)$ only via its dependence on the neutron and proton densities, and thus these options are relevant, and are calculated, only for the radially varying density.

Option 1: Here m is taken as the free mass, E_C =

TABLE III. Radiative capture rates $\Gamma(\geq 57)$ in units of s^{-1} for a variety of nuclei, assuming a uniform nuclear density distribution. A cut has been performed to give photon energies above 57 MeV only. The numbered columns correspond to the various options described in the text. Option 9 is the same as 6 for a uniform density and so is not repeated. The last column gives the relative rate $R(\geq 57)$ in units of 10^{-6} for option 6 (or 9). Nuclei lighter than ^{40}Ca are included for reference only, as our model is not expected to be applicable for such nuclei.

	1	2	3	4	5	6	$R(>57)$
$_{6}$C	2.15	1.30	3.46	3.43	4.17	0.909	18.5
$_{8}$O	6.36	3.86	9.07	8.92	11.6	3.29	22.4
$_{13}$Al	35.4	21.5	36.6	35.1	52.3	33.1	36.8
$_{14}$Si	45.5	27.6	56.5	53.8	81.4	35.6	31.4
$_{20}$Ca	139	84.5	169	153	262	138	37.0
$_{26}$Fe	302	183	200	168	352	176	30.3
$_{28}$Ni	374	227	304	250	539	295	35.5
$_{42}$Mo	995	604	318	201	695	354	25.7
$_{50}$Sn	1386	841	272	139	648	296	20.5
$_{64}$Gd	1988	1206	315	110	760	378	19.6
$_{74}$W	2375	1440	352	93.1	852	390	18.0
$_{82}$Pb	2815	1707	275	49.9	726	249	13.3
$_{83}$Bi	2756	1672	343	65.5	843	452	18.5
$_{92}$U	3074	1865	270	33.9	691	256	12.9

TABLE IV. Radiative capture rates $\Gamma(\geq 57)$ in units of s^{-1} for a variety of nuclei, assuming a two-parameter Fermi-Dirac nuclear density distribution. A cut has been performed to give photon energies above 57 MeV only. The numbered columns correspond to the various options described in the text. The columns labeled by $R(\geq 57)$ give the relative rates in units of 10^{-6} for options 7, 8, and 9. Nuclei lighter than ^{40}Ca are included for reference only, as our model is not expected to be applicable for such nuclei.

	6	7	$R(>57)$	8	$R(>57)$	9	$R(>57)$
$_{6}$C	0.909	1.24	22.6	1.57	25.6	1.52	25.3
$_{8}$O	3.29	4.49	27.0	5.51	30.0	5.30	29.5
$_{13}$Al	33.1	42.8	42.5	48.6	44.8	45.2	43.8
$_{14}$Si	35.6	47.6	36.9	55.7	39.9	51.6	38.8
$_{20}$Ca	138	173	42.5	198	45.2	178	43.5
$_{26}$Fe	176	263	36.5	296	38.5	254	36.5
$_{28}$Ni	295	423	42.1	476	44.3	411	42.0
$_{42}$Mo	354	572	31.1	630	32.5	504	30.2
$_{50}$Sn	296	523	25.2	577	26.4	435	24.1
$_{64}$Gd	378	611	23.5	666	24.6	480	22.1
$_{74}$W	390	659	21.6	730	22.7	526	20.4
$_{82}$Pb	249	463	16.4	512	17.3	344	15.1
$_{83}$Bi	452	700	21.7	756	22.6	547	20.3
$_{92}$U	256	475	16.1	525	17.0	324	14.5

$E_{\mu B} = 0$ and $k_{F_p} = k_{F_n} = 280$ MeV. Under these circumstances $\Gamma(\rho_p, \rho_n)$ in Eq. (7) is a constant and hence the result is independent of the nuclear density. The only dependence on the nucleus is via the overall factor $Z_{\rm eff}^4$, except for a negligible dependence coming from slightly different values of the muon reduced mass. This result reduces to the infinite nuclear matter result of Ref. [9], once account is taken of the appropriate $Z_{\rm eff}$ and the fact that rates were always quoted per proton in that reference.

For this situation both $\Gamma_{\rm OMC}$ and $\Gamma(\geq 57)$ decrease as k_F gets larger, as was found in Ref. [9]. These rates actually vary rather steeply with k_F as can be seen from Fig. 2, where we show this variation with k_F, using for simplicity ^{40}Ca which has $k_{F_p} = k_{F_n}$.

Option 2: The mass is now replaced by $m^* = 0.57m$, taken as a constant calculated from the relativistic mean field theory with $G_S\phi_0 \cong 400$ MeV. This leads to a reduction in the calculated ordinary rate and in $\Gamma(\geq 57)$ again in agreement with Ref. [9]. The radiative and ordinary rates as a function of m^* are given in Fig. 3, and from this we can see that the rates increase almost linearly with increasing m^*. This result is still equivalent to the corresponding infinite nuclear matter rate.

Option 3: k_{F_p} and k_{F_n} are now calculated from the proton and neutron average densities, respectively, which are taken to be the central densities for the uniform distribution. In light nuclei, k_{F_p} and k_{F_n} are very similar

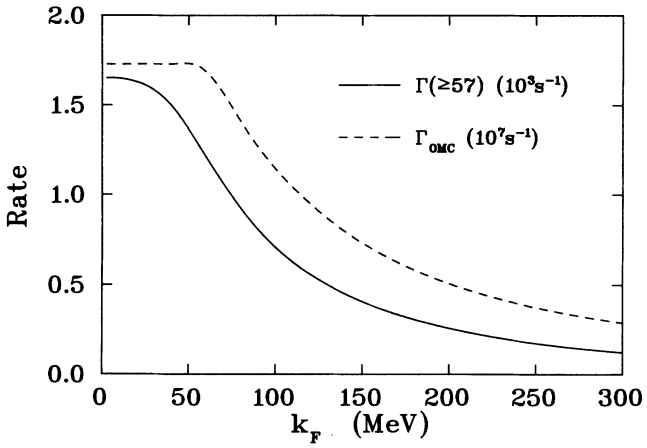

FIG. 2. Variation of the radiative rate $\Gamma(\geq 57)$ in units of 10^3 s^{-1} and the ordinary rate $\Gamma_{\rm OMC}$ in units of 10^7 s^{-1} with the Fermi momentum k_F. The conditions of option 1 of the text have been assumed, i.e., $m^* = m$, $E_{\mu B} = E_C = 0$, $k_{F_p} = k_{F_n}$. The numbers quoted are for ^{40}Ca though are proportional to the infinite nuclear matter result for any $N = Z$ nucleus.

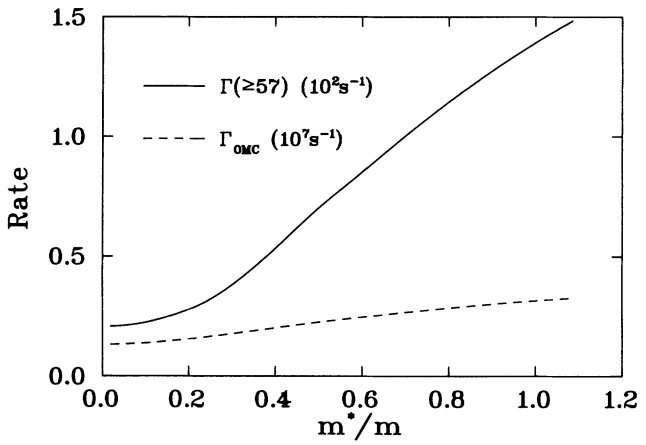

FIG. 3. The radiative rate $\Gamma(\geq 57)$ in units of 10^2 s^{-1} and the ordinary rate $\Gamma_{\rm OMC}$ in units of 10^7 s^{-1} shown as a function of m^* for ^{40}Ca. The parameters of option 2 of the text, namely, $E_{\mu B} = E_C = 0$ and $k_{F_p} = k_{F_n}$=280 MeV, have been assumed. As in Fig. 2 the results quoted for ^{40}Ca are proportional to the infinite nuclear matter rate for any $N = Z$ nucleus.

and significantly smaller than the 280 MeV used in the previous options. Thus both ordinary and radiative rates increase, because of the general increase in rates as k_F becomes smaller. For heavy nuclei however k_{F_n} is substantially greater than k_{F_p}. Since muon capture must occur upon a proton with momentum $p < k_{F_p}$ and result in a neutron with $n > k_{F_n}$, we find a substantial suppression of both the ordinary and radiative muon capture rates in heavy nuclei, amounting to a factor of more than 2.5 for OMC and 6 for RMC for ^{208}Pb in the uniform density model. In that case $k_{F_p} = 233$ MeV and $k_{F_n} = 269$ MeV. This is due to the reduction in allowed phase space for the interaction in these heavy nuclei and the fact that both RMC and OMC are very sensitive to the amount of energy available for the ν and γ.

Option 4: The muon binding energy is included, leading to a reduction in the allowed phase space for the interaction, and a resultant decrease in the rates. The decrease is small for light nuclei where the binding energies are small. For heavy nuclei, however, the binding energies are ~ 10 MeV and the decrease is much larger. This is particularly true for $\Gamma(\geq 57)$ where a 10 MeV shift in the available energy is significant relative to the range of energies, $57 \rightarrow\sim 100$ MeV which is relevant.

Option 5: The Coulomb energy E_C included, also as a constant, calculated from Eq. (11). This enters in the same fashion as the binding energy, but is of opposite sign and generally larger. The rates are increased. What is important is the combination $E_C - E_{\mu B}$, which ranges from about 5 MeV for ^{40}Ca to about 10 MeV for ^{238}U and which corresponds to the additional energy available for the nuclear process as compared to the free case. The net effect of these two is to increase the ordinary rate by 50% or so for heavy nuclei and increase $\Gamma(\geq 57)$ by more than a factor of 2.

Option 6: The additional isospin dependent energy ΔE is included so that the ground state energy separation and the overall maximum photon or neutrino energy are correct. ΔE works in the direction opposite to E_C and cancels typically half or more of the increase in rates which was generated by E_C. In fact the three ingredients, the muon binding energy, the Coulomb energy, and ΔE cancel nearly completely as can be seen by comparing options 3 and 6. This means that neglecting all three is a significantly better approximation than keeping just one or two.

Option 7: The Fermi momenta are made functions of r according to the prescription of the local density approximation, i.e., k_F is calculated from $\rho(r)$ via Eq. (4). This means that for the Fermi-Dirac distribution k_F varies across the nucleus from nearly nuclear matter values in the center to nearly zero in the tail. The rates for heavy nuclei increase dramatically, for reasons which will be discussed below.

Option 8: m^* is put in as a function of k_F and hence as a function of r using a phenomenological fit to the expression derived self-consistently in Ref. [26] from relativistic mean field theory and illustrated in Fig. 4. This increases the rates by a few percent for OMC and roughly 10% for RMC.

Option 9: The muon wave function, calculated by integrating the Schrödinger equation for the Fermi-Dirac $\rho(r)$ as described above, is kept under the radial integration in Eq. (7), and $Z_{\rm eff}$ is replaced by Z. The value of $Z_{\rm eff}$ we calculate from our wave function solutions differs from the more accurate value obtained by Ford and Wills [23] by solving the Dirac equation by at most 2%. However since the rates depend on $Z^4_{\rm eff}$, this leads to a small mismatch between this option and the others. To correct for this we have renormalized our results by the ratio of $Z^4_{\rm eff}$ from Ref. [23] to that we calculated. This changes the rates in the worst case by 10%, but of course does not affect the ratio of RMC to OMC, which is the experimentally relevant quantity.

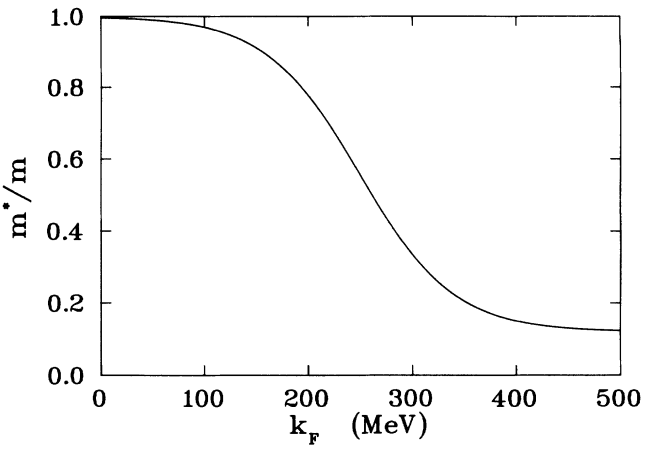

FIG. 4. Dependence of m^* upon the nucleon Fermi momentum k_F, as calculated in mean field theory [26] using the standard Serot-Walecka [13] parameter set.

The introduction of the muon wave function under the integral for the nonuniform density case leads to a rather significant reduction in the rates, for the reasons discussed below.

As one can see from considering these various options there are really two kinds of effects which have strong influence on the results for the final rates. The first type are those effects which change the phase space. This is important because of the well known sensitivity of both OMC and RMC to the end point of the spectrum, i.e., sensitivity essentially to the energy available for the process. These effects include the muon binding energy and the energy ΔE which reduce and the Coulomb energy which increases the amount of energy available for the final particles. This also includes the effects of calculating k_{F_p} and k_{F_n} separately. As the nucleus gets heavier $N - Z$ gets larger and k_{F_n} becomes significantly larger than k_{F_p}. This means more and more momentum is required just to get the neutron above the Fermi sea and that less and less is available for the phase space. The rates for heavy nuclei are therefore strongly suppressed.

The second major effect arises because of the variation of $\Gamma(\rho_p, \rho_n)$ with the radius r. The integrand in Eq. (7) is strongly peaked at the surface of the nucleus because of the r^2 factor. Figure 5 shows $4\pi r^2 \rho_p(r)$ as a function of r. As we add effects which make $\Gamma(\rho_p, \rho_n)$ no longer constant across the nucleus, we change the weighting of

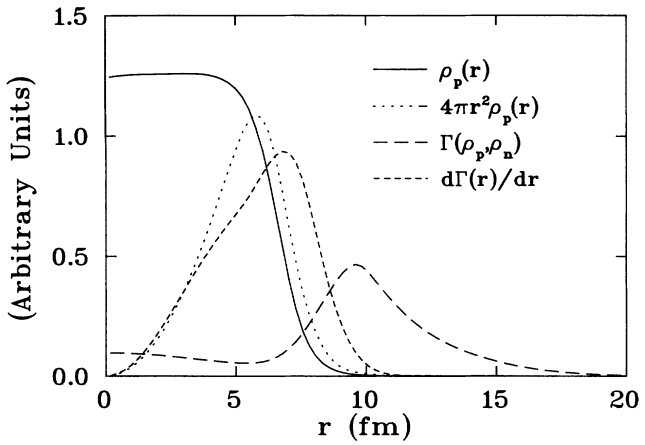

FIG. 5. Components of the integrand of Eq. (7) vs r. Shown is $4\pi r^2\rho_p(r)$ and $\rho_p(r)$, together with $\Gamma(\rho_p,\rho_n)$ and the full integrand $d\Gamma(r)/dr$ for RMC. The plotted results correspond to option 9 for ^{208}Pb, using a Fermi-Dirac distribution. The corresponding quantities for OMC are qualitatively similar.

the integral and can change the rates. For example, making m^* a function of r enhances the rates slightly since $\Gamma(\rho_p,\rho_n)$ increases with m as in Fig. 3 and since $m^* \to m$ in the more highly weighted surface region.

The really dramatic effect comes, however, when we take k_F as a function of density and allow it to vary with the density across the nucleus. This is relevant only for the Fermi-Dirac distribution, but there k_F ranges from nuclear matter values in the center of the nucleus to nearly zero in the surface tail. This becomes important because of the rapid variation of $\Gamma(\rho_p,\rho_n)$ with k_F (see Fig. 2). $\Gamma(\rho_p,\rho_n)$ is then much enhanced in the surface region and this leads, because of the heavy weighting of this region in the integral, to much enhanced overall rates.

It is just this effect, however, which makes it important to put the muon wave function under the integral rather than use $Z_{\rm eff}$ in these circumstances. $Z_{\rm eff}$ is calculated assuming a constant weighting by the $\Gamma(\rho_p,\rho_n)$ factor. If this rate is significantly enhanced in the low density surface region, then the whole integral is weighted toward regions where $|\phi_\mu(r)|^2$ is small and the result is smaller than one would get using $Z_{\rm eff}$.

Some of these considerations are illustrated in Fig. 5 which shows $\Gamma(\rho_p,\rho_n)$, the phase space $4\pi r^2\rho(r)$, and the complete integrand as a function of r. The RMC rate falls off gradually with r near the center of the nucleus as a consequence of the decreasing $|\phi_\mu|^2$. Near the surface, as the density begins to decrease $m^* \to m$ and $k_F \to 0$, and the rates increase dramatically. Then for large r, $|\phi_\mu(r)|^2$ takes over and $\Gamma(\rho_p,\rho_n) \to 0$. The phase space also peaks at the surface, and thus the integrand of Eq. (7) is dominated by the surface region. Similar considerations apply to the OMC rates.

It should be clear from this discussion that there are a number of competing effects which combine to give the final result. Some of these effects change the overall rates by factors of 2 or 3 or more. In option 9 we make what we feel to be the most appropriate and complete choices. However other choices might be possible and could affect the results. Thus it may be very difficult to predict either radiative or ordinary rates with confidence. If one is willing to treat some of the ingredients as free parameters, as has been done in some previous calculations, then it may be very easy to fit any data that becomes available. Such fitting is, however, not an approach we would advocate.

In Fig. 6 are plots of the experimentally accessible photon spectra in the final version of our model (option 9 of Table IV) for a small selection of the studied nuclei—^{40}Ca, ^{112}Sn, and ^{208}Pb. The end point of the photon spectra varies among the nuclei depending on the muon binding energy and ΔM. The shape of the photon spectrum near the end point depends on the details of the calculation and in particular on how the various ingredients are weighted. Figure 6 also shows spectra using the uniform density distribution, normalized to the same value at 60 MeV. One can see that the various r dependent effects we have included and the Fermi-Dirac density distribution give a spectrum which is enhanced near the end point relative to the usual uniform density model. In principle this will affect the extraction of g_P from the experimental data, since it is normally necessary to fold the theoretical spectrum with various experimental resolutions in order to compare with the actual measurements of events.

Examples of the complete photon spectra for ^{208}Pb with differing values of the pseudoscalar coupling constant g_P are shown in Fig. 7.

It is interesting now to compare our results with those of other groups. We are aware of two calculations, those of Chiang *et al.* [20] and of Christillin *et al.* [25], which overlap ours to some extent. In both cases much of the

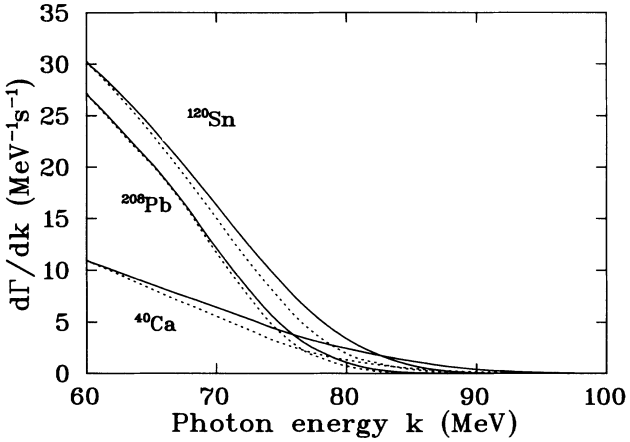

FIG. 6. Photon spectrum $d\Gamma/dk$ for ^{40}Ca, ^{120}Sn, and ^{208}Pb in the experimentally accessible region. We have assumed a Fermi-Dirac distribution, all of the dependences of option 9, and the Goldberger-Treiman value for g_P. The dotted curves are the same quantities calculated using a uniform distribution and normalized to the solid curves at 60 MeV, so as to emphasize the difference in shape near the end point caused by the various density dependent effects we have included.

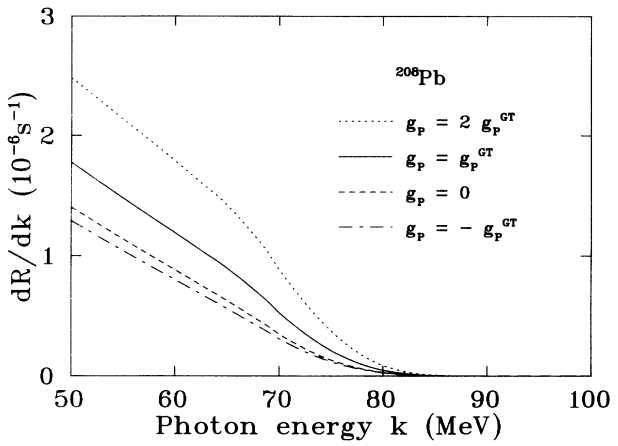

FIG. 7. Relative photon spectra dR/dk, in units of 10^{-6} s^{-1}, for ^{208}Pb as function of g_P. A Fermi-Dirac distribution is assumed and all of the dependences of option 9 of the text. The curves correspond to values of g_P which are 2, 1, 0, and -1 times the Goldberger-Treiman value.

physics motivation and details are quite different. However there are some limiting situations which provide a point of contact and a completely independent check of our results. More importantly, now that we have discussed the dependence of the results on the various ingredients, we are in a position to try to understand the reasons for differences in the final results.

Chiang *et al.* [20] look just at ordinary muon capture and are interested primarily in calculating strong renormalization effects due to particle-hole excitations in the nuclear medium. Their calculation is relativistic and they use the local density approximation, with a Fermi-Dirac charge distribution and a Fermi gas model, just as we do. The muon binding energy is included but E_C and the ΔE correction are not. The muon wave function, calculated nonrelativisticly, is put under the integral. Although not specifically noted, their renormalization effects are almost exactly just an overall constant, 0.54, over the whole range of nuclei considered. Their results agree rather well with a large number of ordinary muon capture rates.

They do, however, give a no renormalization limit of their calculation which can be compared with our no renormalization results, i.e., with our calculation for the Fermi-Dirac distribution, with the muon wave function under the integral and using $m^* = m$, $E_C = 0$, and $\Delta E = 0$. For nuclei over the whole range ^{40}Ca to ^{208}Pb we agree at the 10–20 % level. Our results are a bit lower for the heavy and light nuclei and a bit higher in the middle region. They state that dropping $E_{\mu B}$ gives a 35% effect in ^{208}Pb, which we find as well. Given that some of the parameters may differ somewhat, we interpret this as quite good agreement which gives confidence in the numerical correctness of both calculations.

Their full calculation, as opposed to this limiting case, differs from our full calculation in two major physics respects. First the method of renormalization to account for medium effects is different and produces a reduction of the rates by a factor 0.54, whereas replacing m by m^* in our calculation leads to a reduction of only 20–35 %. Secondly they do not include the Coulomb energy or the ΔE correction, which in principle should be there. Including E_C increases the rates by 20% for ^{40}Ca up to a factor of nearly 2.5 for ^{208}Pb. Including ΔE cancels part of this, as they realized [27], but not all of it as we noted in the discussion of option 6 earlier. Thus one must conclude that the good agreement with experiment which they find must be somewhat fortuitous, especially for heavy nuclei, and would be not as impressive when E_C and ΔE are included. Our best results in this model then are significantly larger than theirs, because of the lesser renormalization and because we have included both the Coulomb energy and ΔE which they have not.

A second calculation by Christillin *et al.* [25] deals with both RMC and OMC in much the same spirit we have done, in that the calculation is based on a Fermi gas model of the nucleus and the local density approximation. It differs however both technically and philosophically in several important aspects. Their calculation is purely nonrelativistic, and even some of the leading p/m corrections have been dropped from the radiative matrix element. They consider only a uniform charge distribution, so that none of the r dependent effects we have discussed are considered. The effective mass m^* is treated as a free parameter and varied in order to fit the OMC data rather than obtained consistently from the relativistic mean field theory as we do. They include $E_{\mu B}$ and in some fashion E_C, but presumedly only in the phase space, whereas in our calculation a consistent application of the relativistic mean field theory (and of gauge invariance) requires some dependence also of the matrix element on these quantities. Apparently the ΔE correction is not included. They include a modification of the Coulomb propagator of the muon, which we do not, but that is supposed to be only a few percent effect [28]. Roughly speaking then their model corresponds to our option 5 for the uniform density model, with a number of relativistic and other corrections dropped and with a different set of parameters, notably $m^* = 0.5m$.

When we compare our results for OMC with theirs, using a uniform density and as near as we can tell the same parameters they used, but keeping all of the relativistic effects, which we cannot separate out, we find results which are higher than theirs by factors ranging from 1.6 for ^{40}Ca to 2.0 for ^{208}Pb. This is rather puzzling in view of our relatively good agreement with Chiang *et al.* [20]. We did find empirically that multiplying our results by the factor $1 - 2.5(N - Z)/A$, which was obtained in Ref. [25] as an approximate overall factor for a simple calculation, does give much better agreement, but see no reason why this should be done.

For RMC the disagreement is even worse as $d\Gamma/dk$ is always larger than theirs by factors of 2–3 at 60 MeV and by as much as a factor of 5 at 75 MeV. We also seem to have (for $\Delta E = 0$) a significantly higher maximum photon energy, and thus a spectrum shape which is enhanced at the upper end as compared to theirs. This latter effect is actually desirable as there appear to be indications in new TRIUMF data on a variety of nuclei [2, 3] of signif-

icantly more events at high energies than predicted by the spectra of Christillin *et al.* [25].

Again we found empirically that if we arbitrarily modify the relation between k_F and ρ, which is given in Eq. (4) by replacing the 3 by 3β where $\beta \approx \frac{5}{3} \approx \pi/2$ is a free parameter, then we agree with the OMC results of Ref. [25] to about 10% and with the RMC results over the range 60–75 MeV to about 25%. This also makes the end point of the spectrum in better agreement. However there is no indication that the authors of Ref. [25] actually made such a replacement and in fact it is clearly incorrect to do so within the context of the Fermi gas model.

Another possibility is that something analogous to our ΔE was included. One of the figures in Ref. [25] does show ΔM explicitly, but the formulas do not include such effects. In any case we tried including ΔE, basically trying option 6 with the other parameters changed to agree with those of Ref. [25]. This does reduce the rate and make the spectrum end points more similar, but still gives OMC rates 25–50 % higher and RMC rates up to a factor of 2 higher than those of Christillin *et al.* [25].

Thus it would appear that our results differ somewhat from those of Ref. [25], even in the limit in which they should be approximately the same, for reasons which are not understood. It is possible that these differences may still be due to unresolved differences in some of the parameters or to the fact that we cannot compare here with quite all of the same approximations. It is also barely conceivable that relativistic effects could be responsible. The p/m effects in the matrix elements are known to be small, say of the order of 10% or less [16]. However relativistic effects in the phase space could affect the maximum photon energy, and thus the rate, because of the extreme sensitivity of the rate to this maximum energy.

Further physics differences arise when we consider our best model, rather than the limiting comparison case, in accordance with the discussions accompanying Tables II and IV, as a result of the r dependent effects and nonuniform density effects which were not included by Christillin *et al.* [25].

VI. DISCUSSION

In this paper we have examined radiative muon capture for a variety of nuclei in a relativistic mean field theory, using the local density approximation and a Fermi gas model for the nucleus. The aim has been to explore the sensitivities to the various ingredients and to get some idea of the reliability of this approach for extracting the value of the induced pseudoscalar coupling g_P from the data.

Perhaps the most important observation is that the results are very sensitive to the various ingredients, even at the factor of 2 level. Two kinds of things are important. Effects which change the phase space, such as Coulomb and nuclear force corrections, the muon binding energy, and the value of m^*, all affect the maximum energy available to the photon and, as is well known, the rates are quite sensitive to this energy. The other important class of effects are those which depend on the density or lead to a radial dependence of the rates. Thus a Fermi-Dirac density gave quite different results from a uniform density. Putting the muon wave function under the integral was also quite important for the nonuniform density.

This extreme sensitivity to the ingredients has a number of practical consequences. First one is led to view with some suspicion calculations which leave out one or more of these ingredients, as has been the case with most previous calculations, though of course one may leave out ingredients which fortuitously cancel. Second it is clear that if one is willing to treat one or more of the ingredients as free parameters, then it should be possible to fit a given set of data. For example, in Ref. [25] the authors got a good fit to a large number of ordinary muon capture data by varying m^*. Finally it should be clear that it is going to be very difficult to extract g_P from experimental data on the rates because of this sensitivity.

Nevertheless it is of some interest to compare our results with the existing data [1–7], bearing in mind that we have no free parameters, but have in each case chosen what seems to be the most correct choice of ingredients.

We see first that our results for both OMC and RMC rates are significantly higher than the data, when the Goldberger-Treiman value of g_p is used. This is consistent with the results of the authors of Ref. [25] who found relative rates too high even when the OMC rates were fitted to the data by varying m^*. In our case it does not seem possible to reduce the rates sufficiently by varying g_P alone. Something else would have to be varied as well. Thus we have to conclude that this model does not do a very good job reproducing the absolute values of the rates.

It is worth noting that there have been theoretical calculations suggesting renormalization of the coupling g_A in nuclear matter. To test the effects of such a renormalization upon our calculated rates, the final version of the model was run for a range of nuclei with $g_A = -1.00$ instead of the usual $g_A = -1.25$. Both the RMC and OMC rates were found to decrease by $\sim 30\%$ for the nuclei tested, with the ratio of RMC to OMC rate being almost unchanged. Clearly this is not a sufficient reduction to provide a good fit to data.

It is interesting to see if any of the other qualitative features of the data are reproduced. As noted above and illustrated in Fig. 6, the various density dependent effects we have introduced do seem to enhance the spectrum in the end point region relative to the uniform density calculation. This seems to be an effect seen in the recent TRIUMF data [2, 3].

We can also look at the trend of the radiative rates with Z. The relative rate is plotted versus Z in Fig. 8 where we have renormalized by a factor of approximately 0.4 to fit the data. The data show a steady decrease with Z of the relative rate $R(\geq 57)$ which is reproduced rather well by the theory for nuclei above ^{40}Ca, the major exception being ^{209}Bi, which is too high. Figure 9 shows the radiative rate $\Gamma(\geq 57)$ plotted versus Z. The data points are obtained by multiplying the measured relative radiative rates by the nonradiative muon capture rates obtained in separate experiments [24]. Again the theoretical calculation does a good job of reproducing the Z dependence

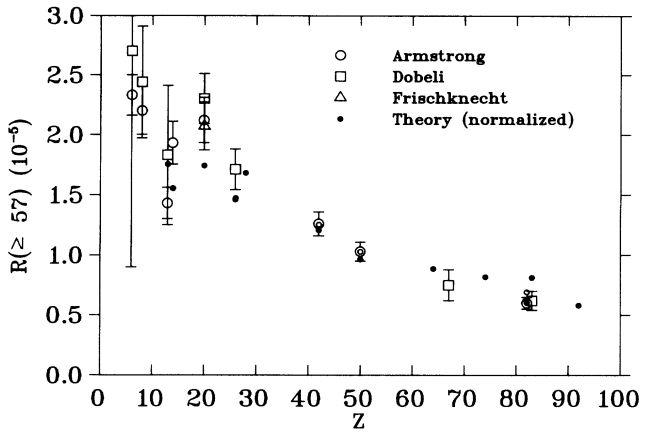

FIG. 8. The relative rate $R(\geq 57)$ as calculated using the dependences of option 9, a Fermi-Dirac distribution, and the Goldberger-Treiman value of g_P plotted vs Z. The overall normalization has been adjusted to fit the data which comes from Refs. [1–7]. The small open circles are estimates for the rates in the natural isotopic mixtures actually measured. Results for nuclei lighter than ^{40}Ca have been included for reference only, as our model is not expected to be applicable to such light nuclei.

of the data (except for ^{209}Bi) once one adjusts the normalization, this time by a factor of approximately 0.2. It should be emphasized that the various ingredients of our best approach, option 9, have been used without modification to get these results. Only the normalization has been varied.

It is interesting to note that even in a model such as the Fermi gas model which essentially averages over almost all properties of the nucleus, some evidence of nuclear structure remains. The difference in the theoretical rates for ^{208}Pb and ^{209}Bi is due almost entirely to the difference in ΔM. In fact using the ΔM for ^{208}Pb in the ^{209}Bi calculation gives results almost identical to those for ^{208}Pb. This results because ^{208}Pb is particularly tightly bound

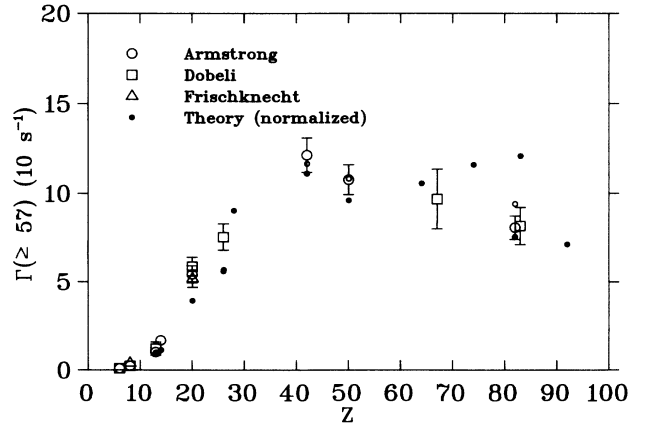

FIG. 9. Same as Fig. 8 except that the rates plotted are the absolute radiative rates. The experimental data are obtained by multiplying the quoted relative rates by ordinary capture rates obtained in separate experiments [24].

so that the energy gap to the ground state of the neighboring nucleus, ΔM, is larger than average for ^{208}Pb and smaller than average for ^{209}Bi. This makes more (less) phase space available for ^{209}Bi (^{208}Pb) and so enhances (suppresses) the rates. The differences between ^{58}Ni and ^{56}Fe appear to come from the same effect.

Note also that this sensitivity to ΔM may affect our comparison with experiment to some extent as we have calculated rates for pure isotopes, whereas some of the experimental data is for the naturally occurring mixture of isotopes. The small open circles in Fig. 8 and Fig. 9 show our estimate of the rates for the natural mixtures which were actually measured. The effect is small for all but Pb.

Another effect should be considered for precise comparisons with experiment. In heavy nuclei of nonzero spin there is a very rapid transition to the lower hyperfine state [24], so that the measured transition is probably predominately from that state rather than from a statistical mixture of spin states as was assumed in our calculations.

One of the interesting physical questions deals with the possible quenching of g_P in heavy nuclei. This could show up in data which fell with increasing Z significantly faster than theoretical calculations would predict using a fixed value of g_P. It has been difficult to address this question in the past because it was necessary to compare data with different calculations, having different inherent normalization uncertainties, for the light nuclei and for the heavier nuclei. Ours is the first that spans the whole Z range, though admittedly some of the approximations are much better for the heavier nuclei. As is clear from Fig. 8 our results show no real evidence for such quenching as a function of Z. It should be emphasized that by quenching we mean some effect which leads to a departure from the form of the Goldberger-Treiman relation. As we use m^* in Eq. (3) the effective numerical value of g_P is reduced from the usual value quoted, $g_p \approx 7g_A$, even though the form and physics of the Goldberger-Treiman relation are preserved. Quenching effects which are more or less the same for all nuclei above ^{40}Ca and which thus could affect the overall normalization are of course not ruled out. In our opinion, because of the sensitivity of the model to the ingredients, any real conclusion about quenching is premature.

Thus, to summarize the important points of this discussion, we note that we have used the relativistic mean field theory in a very simple form to calculate RMC in nuclei. We find sensitivity to a large number of effects, particularly those which change the phase space or depend on the density and conclude from this that one should interpret with some care results for RMC or OMC in variants of this model which do not include *all* of these ingredients. The complete model was then applied to RMC and results compared with recent experiments. The absolute values of the rates are not well reproduced. However the Z dependence seems to be qualitatively correct over a wide range of Z. This suggests that further Z dependent quenching effects, which had been suggested to explain the falloff of the rates with Z, are not necessary. Finally it is clear that to make further quantitative progress and

in particular to extract accurate values of g_P from existing data one will have look at more sophisticated models.

ACKNOWLEDGMENTS

This work was supported in part by a grant from the Natural Sciences and Engineering Research Council of Canada. One of the authors (H.W.F.) would like to acknowledge the hospitality of the Institute for Nuclear Theory at the University of Washington where some of this work was done. The authors would also like to thank D. Armstrong, M. Hasinoff, and A. Serna for providing their data prior to publication and C. Bennhold, C. S. Bohun, J. Deutsch, and E. Oset for some very useful discussions.

[1] D. S. Armstrong *et al.*, Phys. Rev. C **40**, R1100 (1989); **43**, 1425 (1991).
[2] A. Serna, Ph.D. thesis, Virginia Polytechnic Institute, 1991, Phys. Rev. C (unpublished).
[3] D. Armstrong *et al.*, Phys. Rev. C **46**, 1094 (1992).
[4] C. J. Virtue, Ph.D. thesis, University of British Columbia, 1987 (unpublished).
[5] A. Frischknecht *et al.*, Phys. Rev. C **32**, 1506 (1985).
[6] A. Frischknecht *et al.*, Phys. Rev. C **38**, 1996 (1988).
[7] M. Döbeli *et al.*, Phys. Rev. C **37**, 1633 (1988).
[8] D. H. Wright *et al.*, in *Intersections Between Particle and Nuclear Physics*, Tucson, Arizona, 1991, edited by W. T. H. van Oers, AIP Conf. Proc. No. 243 (AIP, New York, 1992), p. 789.
[9] H. W. Fearing and G. E. Walker, Phys. Rev. C **39**, 2349 (1989).
[10] M. Gmitro *et al.*, Nucl. Phys. **A507**, 707 (1990).
[11] F. Roig and J. Navarro, Phys. Lett. B **236**, 393 (1990).
[12] M. Gmitro and P. Truöl, Adv. Nucl. Phys. **18**, 241 (1987), and references cited therein.
[13] B. D. Serot and J. D. Walecka, in *Advances in Nuclear Physics*, edited by J. W. Negele and E. Vogt (Plenum, New York, 1986), Vol. 16.
[14] H. P. C. Rood and H. A. Tolhoek, Nucl. Phys. **70**, 658 (1965).
[15] H. W. Fearing, Phys. Rev. C **21**, 1951 (1980).
[16] R. S. Sloboda and H. W. Fearing, Nucl. Phys. **A340**, 342 (1980).
[17] D. S. Beder and H. W. Fearing, Phys. Rev. D **35**, 2130 (1987).
[18] D. S. Beder and H. W. Fearing, Phys. Rev. D **39**, 3493 (1989).
[19] M. L. Goldberger and S. B. Treiman, Phys. Rev. **111**, 354 (1958).
[20] H. C. Chiang, E. Oset, and P. Fernandez de Cordoba, Nucl. Phys. **A510**, 591 (1990).
[21] C. W. de Jager, H. de Vries, and C. de Vries, At. Data Nucl. Data Tables **14**, 479 (1974).
[22] *Nuclear Physics and Technology*, edited by H. Schopper (Springer, Berlin, 1967), Vol. 2.
[23] K. W. Ford and J. G. Wills, Nucl. Phys. **35**, 295 (1962).
[24] T. Suzuki, D. F. Measday, and J. P. Roalsvig, Phys. Rev. C **35**, 2212 (1987).
[25] P. Christillin, M. Rosa-Clot, and S. Servadio, Nucl. Phys. **A345**, 331 (1980).
[26] J. F. Dawson and J Piekarewicz, Florida State University Report No. FSU-SCRI-91-09, 1991.
[27] E. Oset, private communication.
[28] P. Christillin, M. Rosa-Clot, and S. Servadio, Nucl. Phys. **A345**, 317 (1980).